Tectonophysics 846 (2023) 229654

Contents lists available at ScienceDirect

Tectonophysics

journal homepage: www.elsevier.com/locate/tecto

Post-5 Ma rock deformation on Alonnisos (Greece) constrains the propagation of the North Anatolian Fault

Kristóf Porkoláb [a,b,*], Ernst Willingshofer [a], Dimitrios Sokoutis [a,c], Eszter Békési [a,b], Fred Beekman [a]

[a] Department of Earth Sciences, Utrecht University, Utrecht, Netherlands
[b] Institute of Earth Physics and Space Science, Sopron, Hungary
[c] Department of Geosciences, University of Oslo, Oslo, Norway

ARTICLE INFO

Keywords:
Transform fault propagation
Fault reactivation
Post-Messinian rock deformation
North Anatolian Fault
Northern Sporades
Alonnisos

ABSTRACT

The localization of the North Anatolian Fault in the northern Aegean Sea (North Aegean Trough) is an intriguing example of continental transform fault propagation. Understanding this process critically depends on the quantification of strike-slip displacement and the superposition of normal and strike-slip faulting in the region, which is the aim of this study. In particular, we unravel and quantify normal and dextral faulting along the Alonnisos fault system, at the south-western margin of the North Aegean Trough (Sporades Basin). We present detailed structural data collected from Messinian strata of Alonnisos to infer the amount of post-5 Ma tilting and shortening on the island, and relate them to normal and dextral faulting along the Alonnisos fault system through simple analytical half-space models of dislocations. The Messinian rocks of Alonnisos record significant (13.5°) tilting and gentle folding close to the termination zone of the main fault segment. The tilting of the Messinian rocks was related to footwall uplift during normal faulting (in the order of 6–7 km vertical displacement) along the Alonnisos fault system, which implies that the deepening of the Sporades Basin occurred post-5 Ma. The post-Messinian folding accommodated ~1 km shortening along the footwall termination zone of the Alonnisos fault and was related to 3–4 km dextral slip, possibly during the last 100–200 kyr. This is the first clear indication of major dextral displacement along the Alonnisos fault system. Our results support interpretations of currently distributed dextral strain in the North Aegean in response to the propagation of the North Anatolian Fault. However, similarities with the evolution of the Sea of Marmara might suggest that dextral shear could yet become fully localized in the NAT.

1. Introduction

The North Aegean Trough (NAT, Fig. 1b) in the northern Aegean Sea is a key region for investigating the interplay between back-arc extension and strike-slip faulting, related to the combined effects of the Hellenic slab-rollback and the westward extrusion of Anatolia (Le Pichon et al., 1981; Lybéris, 1984; Mascle and Martin, 1990; Philippon et al., 2014; Beniest et al., 2016; Sakellariou et al., 2016; Ferentinos et al., 2018). The latter has been accommodated by a major continental transform fault, the North Anatolian Fault (NAF, Fig. 1a), which formed during the Middle Miocene (13–11 Ma, Şengör et al., 2005) in Eastern Turkey, and propagated to Western Turkey where it became fully localized between 5 and 2.5 Ma (Armijo et al., 1999; Le Pichon et al., 2016). Its propagation into the NAT occurred even later, probably during the Early-Middle Pleistocene, and by the reactivation of pre-existing faults that define the south-eastern border of the NAT. Due to this reactivation of pre-existing structures, the NAF changes its strike from ENE-WSW to NE-SW at the NAT (Fig. 1a, Lybéris, 1984; Lyberis and Sauvage, 1985; Roussos and Lyssimachou, 1991; Beniest et al., 2016). In Turkey the NAF is a well-defined and well-documented fault zone with quantified (~ 80 km at the Sea of Marmara) dextral displacement (Barka, 1992; Armijo et al., 1999; Hubert-Ferrari et al., 2002; Şengör et al., 2005).

In contrast, the continuation of the NAF in the Aegean displays distributed, transtensional style of deformation, possibly related to the interaction of the propagating dextral NAF with the pre-existing extensional stress field and fault pattern of the Aegean region (Armijo et al., 1996; McNeill et al., 2004; Philippon et al., 2014; Sakellariou et al.,

* Corresponding author at: Department of Earth Sciences, Utrecht University, Utrecht, Netherlands.
E-mail address: porkolab.kristof@epss.hu (K. Porkoláb).

https://doi.org/10.1016/j.tecto.2022.229654
Received 2 March 2022; Received in revised form 18 August 2022; Accepted 16 November 2022
Available online 23 November 2022

2016; Ferentinos et al., 2018). The Aegean extension is related to trench retreat since ca. 45 Ma, following the stacking of the continental Pelagonian and Rhodopia nappes, which sutured the oceanic Vardar nappe between them (Fig. 1a, Brun and Sokoutis, 2007; Jolivet and Brun, 2010; Brun et al., 2016). The velocity of slab-rollback accelerated substantially due to the Middle Miocene tearing of the Hellenic slab, eventually leading to distributed, whole Aegean-wide extension and basin development (Jolivet et al., 2013; Brun et al., 2016). The currently observed superposition of dextral and extensional faulting in the North Aegean makes the identification of fault segments that represent the true continuation of the NAF much more difficult. Nevertheless, the NAT is recognized as an active strike-slip deformation zone, which defines the boundary between coherently deforming regions (microplates or microblocks) within the Aegean (McKenzie, 1972; Armijo et al., 1996; McClusky et al., 2000; Nyst and Thatcher, 2004).

A key area where the propagation of the NAF can be constrained is the south-western corner of the NAT, the Sporades Basin (e.g. Ferentinos et al., 2018), and the neighbouring Northern Sporades islands (Fig. 1b). The Sporades Basin is a major depression with current water depths of up to 1600 m and largely filled by Neogene and Quaternary sediments. The basin is situated NE from the island of Skopelos and NW from the island of Alonnisos (Fig. 1b). It is generally accepted, that extensional and strike-slip faulting is superposed in the basin, and that recent strike-slip activity is probably related to the propagation of the NAF into the Sporades Basin (Roussos and Lyssimachou, 1991; Hatzfeld et al., 1999; Beniest et al., 2016; Sakellariou et al., 2016; Ferentinos et al., 2018). The interpretation of current dextral movement in the Sporades Basin is further evidenced by dextral earthquake focal mechanism solutions (Fig. 1b, e.g. Hatzfeld et al., 1999; Kiratzi, 2002; Kiratzi and Louvari, 2003; Kassaras et al., 2020) and GPS data (e.g. Hollenstein et al., 2008), which show significant westward motion of the Northern Sporades with respect to the Chalkidiki peninsula (Fig. 1b). Furthermore, GNSS data show that the island of Alonnisos is moving towards the SW 7 mm/yr faster (calculated parallel with the N 40° - N 220° f1 fault, Fig. 1b) than

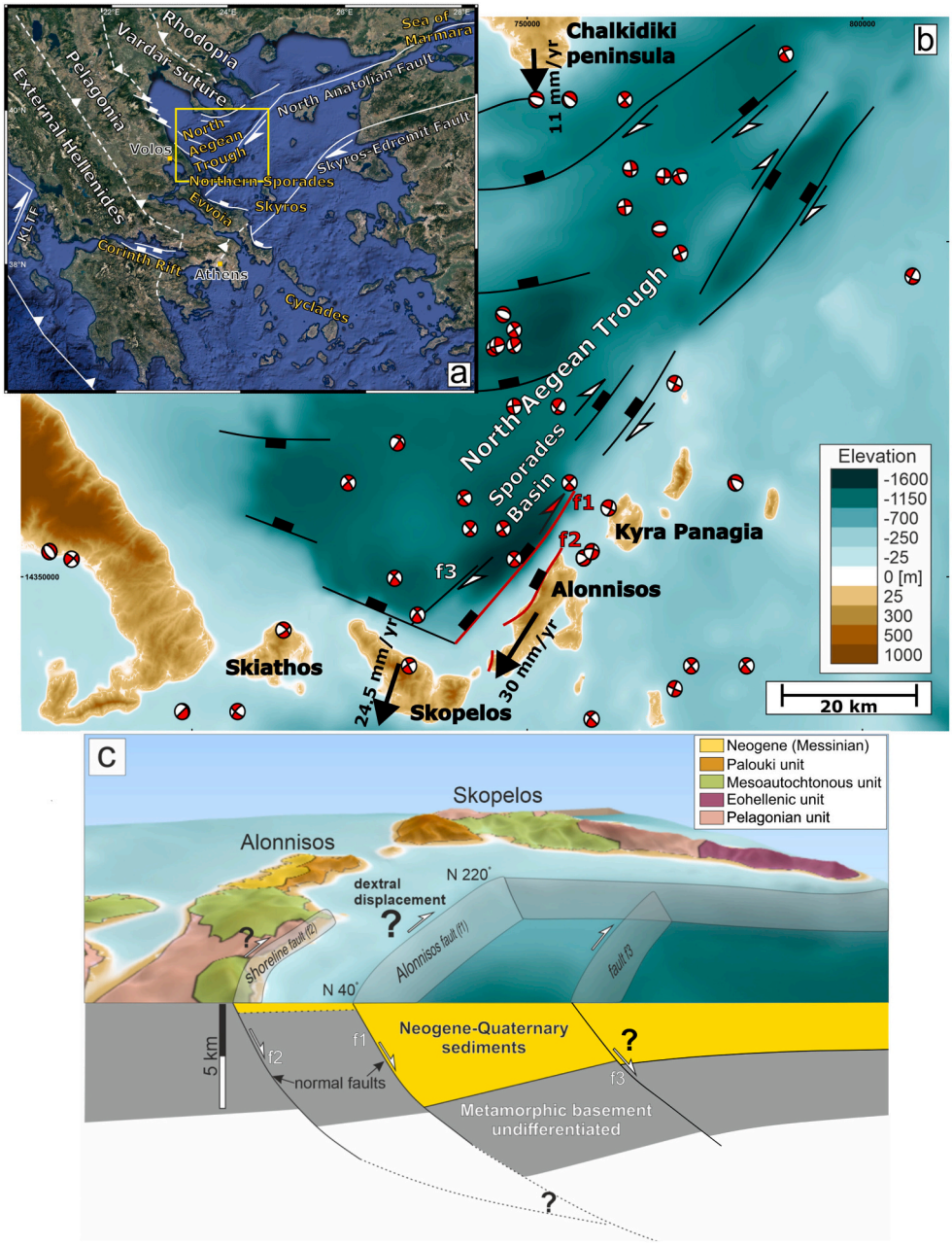

Fig. 1. **(a)** Satellite image of Greece highlighting the main tectonic units, faults and geographic locations. KLTF = Kephalonia - Lefkada transform fault. **(b)** Elevation map and major faults of the North Aegean Trough (NAT). Fault kinematics are based on Ferentinos et al. (2018). The studied Alonnisos fault system (f1 and f2) is highlighted with red colour. Earthquake focal mechanisms data 1900 and 2019 are based on Kapetanidis and Kassaras (2019); GPS data are taken from Hollenstein et al. (2008). SpB = Sporades Basin. **(c)** Schematic 3D structural model of the Sporades Basin and the Alonnisos fault system. Fault geometries are estimated based on Ferentinos et al. (2018). Notice the bathymetry scale that shows the displacement of the seafloor in the hangingwall of the Alonnisos fault by >1000 m, which is not reflected visually in the cross section. (For interpretation of the references to colour in this figure legend, the reader is referred to the web version of this article.)

Skopelos, implying that dextral slip on the f1 fault (from this point called Alonnisos fault, Figs. 1b, c) might be active. However, no clear evidence for major dextral slip on the Alonnisos fault has been presented so far. Earthquake data do record dextral events in the vicinity of the Alonnisos fault, but largely on smaller faults inside the basin (e.g. near the f3 fault, Fig. 1b), or at the island of Kyra Panagia, NE from Alonnisos (Kapetanidis and Kassaras, 2019; Kassaras et al., 2020). In contrast, the extensional origin of the basin is clearly evidenced by the up to 6 km normal-sense displacements along the Alonnisos fault and its north-eastern continuation as well as the thick Neogene sediments in the Sporades Basin (Brooks and Ferentinos, 1980; Mascle and Martin, 1990; Sakellariou et al., 2016; Ferentinos et al., 2018, Fig. 1c). Despite recent progress in mapping the fault geometry and kinematics of the Sporades Basin (Sakellariou et al., 2016; Ferentinos et al., 2018), its spatial and temporal evolution remains poorly constrained. In particular, the superposition of normal and dextral faulting as well as the quantification of the strike-slip component related to the propagation of the NAF are key questions that are still unclear.

We aim at characterising and quantifying deformation related to the superposition of normal and dextral faulting along the Alonnisos fault system (f1 and f2, Figs. 1b, c) in order to constrain fault kinematics related to the propagation of the NAF into the Sporades Basin. To this end, we present detailed structural data collected from the Messinian rocks of Alonnisos. We quantify the deformation (tilting and folding) of the Messinian strata and relate it to normal and dextral faulting along the Alonnisos fault system through simple structural considerations and analytical models of a fault dislocation in an elastic half-space (Okada, 1985; Nikkhoo et al., 2016). The results are interpreted and discussed in the context of the NAF propagation and the interplay between Aegean back-arc extension and the lateral extrusion of Anatolia.

2. Geological background

The islands of the Northern Sporades predominantly consist of

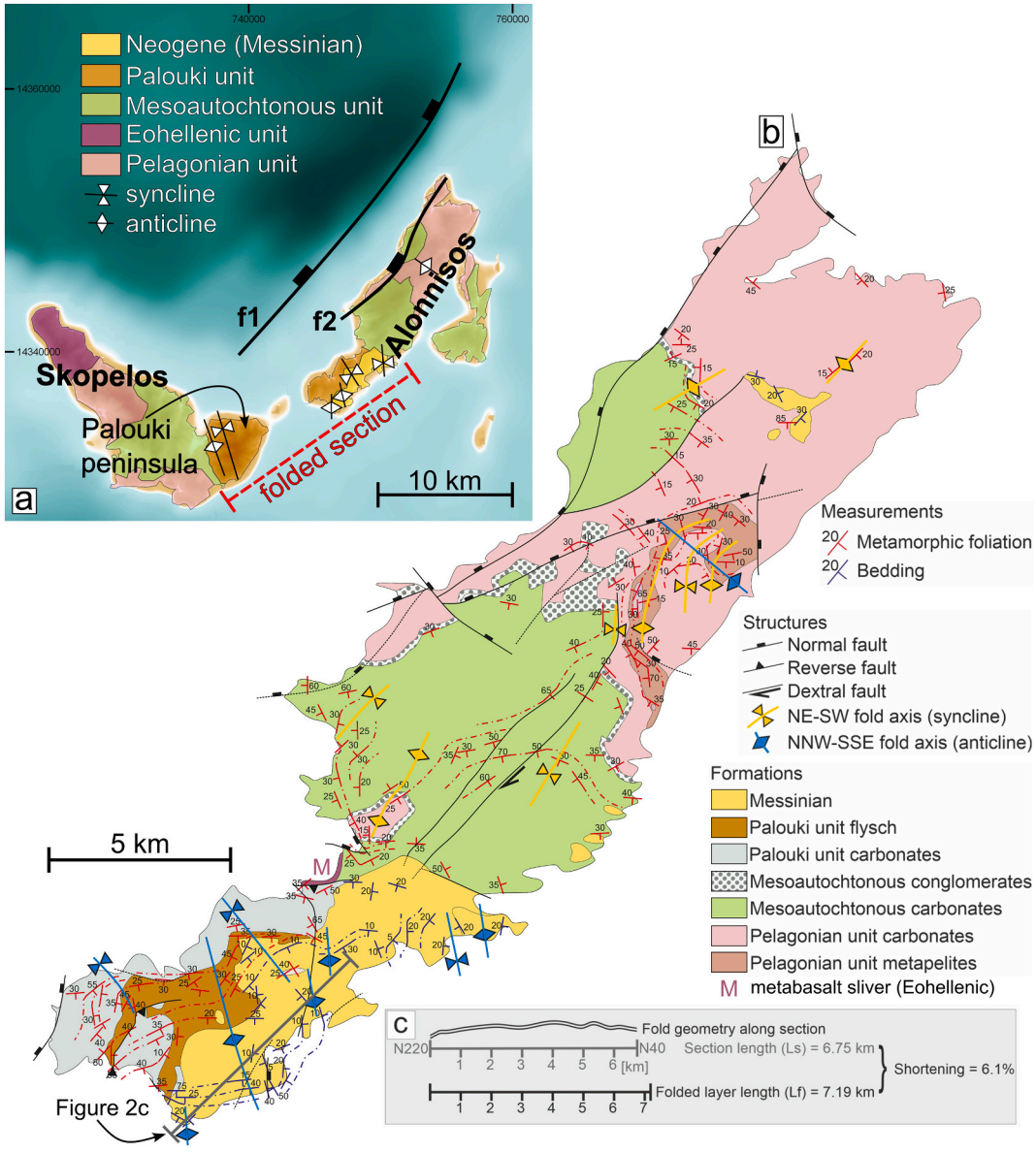

Fig. 2. Geological map of the study area. **(a)** Geological formations of Skopelos and Alonnisos, highlighting the main faults and the area affected by post-Messinian folding. The folded section is ca. 20 km long, and is located at the termination zone of the Alonnisos fault (f1). **(b)** Geological map of Alonnisos modified after Kelepertsis (1974), showing detailed structural data in terms of faults, foliation measurements, and fold axes. **(c)** Line-length balancing of a representative 6.75 km long section across the Messinian strata that implies shortening of around 6%.

Palaeozoic to Eocene, low-grade metamorphic rocks of the Pelagonian zone (Jacobshagen and Wallbrecher, 1984; Jacobshagen and Matarangas, 2004). These are from bottom to top the metapelites and carbonates of the Pelagonian unit, the Eohellenic unit, the Mesoautochtonous unit, and the Palouki unit (Fig. 2b, Kelepertsis, 1974; Jacobshagen and Wallbrecher, 1984; Matarangas, 1992; Jacobshagen and Matarangas, 2004). These formations were buried in an accretionary wedge during latest Cretaceous to Eocene times, and subsequently exhumed along extensional shear zones and normal faults (Porkoláb et al., 2019). Normal faulting on top of the accretionary wedge probably initiated in the late Eocene (Porkoláb et al., 2020) and has been active ever since, contributing to the formation of the NAT (e.g. Beniest et al., 2016; Ferentinos et al., 2018). Seismic interpretations show a thick Neogene basin fill (up to 4–5 km in the Sporades basin, Sakellariou et al., 2016; Ferentinos et al., 2018) that wedges out towards the northern margin of the asymmetric NAT (Fig. 1c). The steep southern margin is defined by fault segments with up to 6 km of normal-sense displacement (Ferentinos et al., 2018), also defining the shoreline of Alonnisos (Figs. 1b, c). Paleogene deposits lying directly on the metamorphic basement are present in the north-western Thermaikos Basin, however, the extrapolation of such deposits into the Sporades Basin is to be confirmed by boreholes (Beniest et al., 2016; Varesis and Anastasakis, 2021).

Alonnisos is the only island of the Sporades that display Neogene sedimentary rocks, which unconformably cover the metamorphic rocks of the Palouki and Mesoautochtenous units (Fig. 1c, Fig. 2). These rocks consist of shallow-water carbonates (Fig. 3b) and up-section alluvial fan conglomerates (Fig. 3c) that are preserved on the SW-part of Alonnisos (Fig. 2b). The stratigraphic age is dated as Upper Miocene based on fossils (Kelepertsis, 1974), and more precisely interpreted to be Messinian based on stratigraphic correlation (Poulimenos and Karkanas, 1998).

3. Data collection and methods

3.1. Field work

Geological field work was conducted on Alonnisos and, subordinately, on the Palouki Peninsula of Skopelos (Fig. 2a). Structural mapping focused particularly on measuring sedimentary bedding planes in the Messinian strata, metamorphic foliations in the Paleogene and older formations (Fig. 2b), (map-scale) fault (slickensides and slickenlines, Riedel shears) and fold structures. The mapping resulted in the revision of the geological map of Alonnisos (Kelepertsis, 1974, Fig. 2b). The new map contains 162 bedding/metamorphic foliation measurements, which includes 37 measurements taken from the map of Kelepertsis (1974) and 125 new measurements. This dataset allowed to establish map-scale fold patterns (Fig. 2b). Mapping and structural analysis were especially focused on the Messinian sedimentary rocks outcropping on Alonnisos in order to characterise the relatively young deformation affecting the area.

3.2. Dislocation modelling

In order to quantify and relate the deformation of the Messinian strata to fault activity along the Alonnisos fault system, we conducted a model parameter study using the compound dislocation model (CDM) method (Okada, 1985; Nikkhoo et al., 2016), which is based on elastic dislocation theory and allows to quantify the surface response of a half-space model to an imposed displacement along a dislocation (fault). We approximated movements along the Alonnisos fault system with a single rectangular dislocation assuming uniform slip. We calculated the surface movements related to slip along the rectangular dislocation using the MATLAB-based function of Nikkhoo et al. (2016). Varied model parameters were the vertical slip component, dextral slip component (rake), fault dip angle, and the Poisson's ratio of the half-space (for more details see the Model Setup and Model Results sections).

4. Results

4.1. Structural results

Based on field observations, we identified two map-scale, gentle to open fold populations. The first population is NE-SW trending, and was not detected in the Messinian rocks, while the second one is NNW-SSE trending, and is especially well-developed in the Messinian strata outcropping on SW-Alonnisos (Fig. 2). This fold population was also observed on the Palouki peninsula of Skopelos (SE-Skopelos, Fig. 2a).

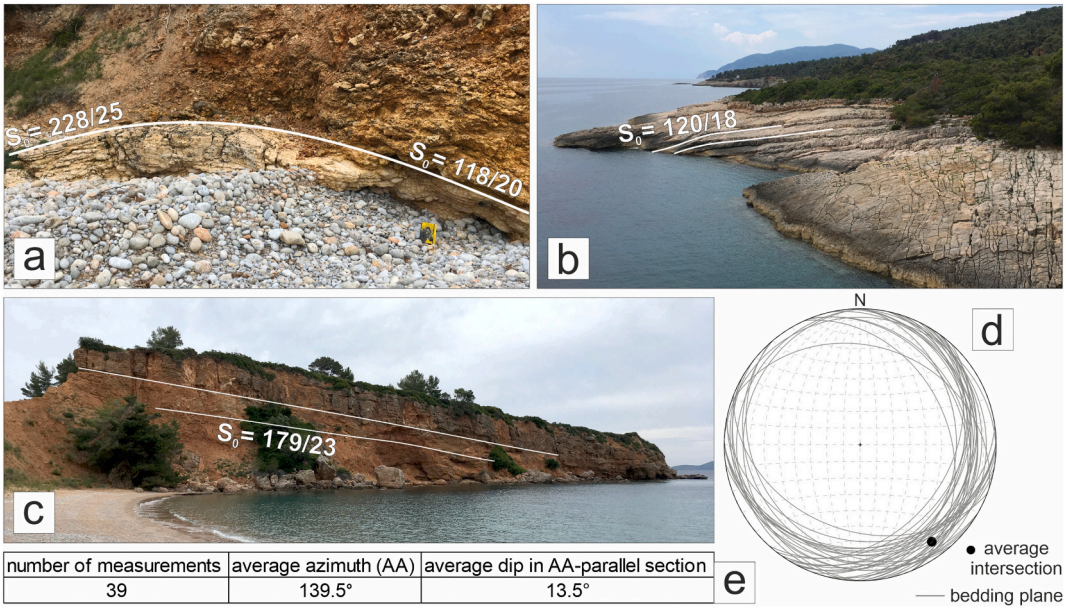

number of measurements	average azimuth (AA)	average dip in AA-parallel section
39	139.5°	13.5°

e

Fig. 3. Field photographs and bedding measurements of the Messinian strata on Alonnisos. **(a)** Hinge of a gentle fold where the Messinian carbonates transition into siliciclastic conglomerates. **(b)** SE-dipping carbonate beds. **(c)** S-dipping conglomerate beds. **(d)** Stereographic projection of the bedding measurements. **(e)** Data of the bedding measurements. The average dip (or tilt angle) of the Messinian strata towards the average azimuth (139.5°) is 13.5°.

We note the presence of some minor outcrop-scale normal and reverse faults affecting the Messinian rocks (also reported by Poulimenos and Karkanas, 1998), but the overall displacement accommodated by these structures is negligible on the scale of the island.

We further revised the location and kinematics of map-scale faults (Fig. 2b), which are dominantly NE-SW trending normal faults that are subparallel with the Alonnisos fault system (f1 and f2, Figs. 1b, c). The largest onshore structure is a normal fault running parallel to the shoreline (f2), which has produced the steep and spectacular fault scarp of Alonnisos with a vertical displacement of at least 500 m (Fig. 1c). The maximum displacement could possibly exceed 1 km, but is not constrained by observations.

4.1.1. Tilting of the Messinian strata

Measurements of sedimentary bedding in the Messinian rocks of Alonnisos (Figs. 2b, 3) have been subjected to a selection procedure, where we eliminated the locally disturbed data (e.g. bedding planes locally steepened by a fault) from the representative population of orientation data. The resulting dataset consists of 39 bedding plane measurements, with an average dip azimuth of N 139.5° (trending N 49.5°) and an average dip angle of 13.5°, calculated for a section that is parallel to the average azimuth (Figs. 3d, e). This clearly indicates that the Messinian strata are significantly tilted around an axis that is subparallel with the Alonnisos fault, which trends ~ N 40°. The Messinian strata are eroded from most parts of Alonnisos, therefore the gradient of the tilting steepness across the island is not clear. The metamorphic foliation of the pre-Messinian rocks also has a dominant SE-dip (Fig. 2b). However, we did not use these data for estimating the tilt angle due to the multiple folding and shearing events (e.g. Porkoláb et al., 2019) that disturb the signal of the post-Messinian tilting in these formations.

4.1.2. Folding of the Messinian strata

The analysis of bedding plane orientations show that the Messinian sediments are gently folded around NNW-SSE trending axes (Figs. 2b, c and Fig. 3a). These fold axes are not exactly perpendicular, but slightly oblique to the Alonnisos fault (Fig. 2a). This fold population is best developed in the Messinian sediments on SW-Alonnisos, and are largely absent from the central and eastern parts of the island (Fig. 2b). A fold population with identical interlimb angles and orientation was observed on the Palouki peninsula of Skopelos, but is absent from the rest of the island (Fig. 2a, for a detailed structural map of Skopelos see Porkoláb et al., 2019). This suggests that the area which is affected by this folding event is 15–25 km long, and overlaps with the termination zone of the Alonnisos fault (Figs. 1, 2a). The amount of shortening for this folding phase has been estimated by line-length balancing of a representative, 6.75 km long, fault-parallel (N 40°) section in the Messinian sediments (Fig. 2c). The balancing estimation shows that the gentle folding accommodated ~6% fault-parallel shortening, which equals 0.9 to 1.5 km shortening over a distance of 15 to 25 km, respectively (considering the approximate length of the folded section, Fig. 2a). Other structures that would have accommodated significant amounts of fault-parallel, post-Messinian shortening, such as major reverse faults, were not observed.

4.2. Structural interpretation and model considerations

The interpretation of structural observations (tilting and folding) was used to design and constrain an elastic compound dislocation model (CDM). Firstly, we interpret the fault-parallel tilting of the Messinian sediments as a result of footwall uplift in response to normal faulting, as described by Weissel and Karner (1989), observed for example at the Corinth Rift (Armijo et al., 1996; de Gelder et al., 2019). We used the CDM to test whether 1) this interpretation was realistic for the Alonnisos fault system, and 2) which fault parameters exert a major control on the tilting in the footwall.

Secondly, we assume that all post-Messinian, fault-parallel shortening of ca. 900–1500 m was accommodated by gentle folding around NNW-SSE trending axes close to the termination zone of the Alonnisos fault (f1, Fig. 1), on SW-Alonnisos and SE-Skopelos (Fig. 2a). The fold axes are not precisely perpendicular, but slightly oblique to the Alonnisos fault, resembling an en-echelon fold arrangement in a dextral strike-slip deformation zone (Fig. 2a). In addition, there is no continuation or linking structure observed at the termination of the Alonnisos fault, meaning that any lateral slip on the fault should result in rock deformation at the termination zone. Hence, we interpret the post-Messinian shortening at the termination zone of the Alonnisos fault as the consequence of dextral slip on the Alonnisos fault or fault system (f1 fault and possibly also the f2 fault, Fig. 1), i.e. the southwest directed motion of the footwall. We used the CDM for quantifying the amount of dextral slip component required for producing 900–1500 m lateral footwall motion, which in nature could be accommodated by folding at the fault termination zone.

4.3. Model setup

The fault geometry was estimated using available reflection seismic data (Sakellariou et al., 2016; Ferentinos et al., 2018). The Alonnisos fault is almost straight in nature, and can thus be approximated by a 30 km long straight fault plane. In contrast, it appears to have varying dip angles along strike ranging from around 70° to 50° with a listric continuation in depth (Ferentinos et al., 2018). Other faults of the Sporades Basin that are in the vicinity of the main Alonnisos fault segment typically dip around 60° (Sakellariou et al., 2016; Ferentinos et al., 2018), including the major normal fault that defines the steep north-western scarp of the island (f2, Fig. 1c, Figs. 2a, b). This fault is only 4–5 km away from and perfectly parallel with the Alonnisos fault (Figs. 1c, 2a), insinuating a connection at depth (Fig. 1c), similar to the basin-bounding faults in the northeastern part of the NAT (McNeill et al., 2004). For these reasons, we treat the f1 and f2 as parts of the same fault system (Alonnisos fault system), and approximate them as a single dislocation plane in our models. The vertical (normal) displacement component of the Alonnisos fault (f1) appears to be around 6 km on seismic lines (Ferentinos et al., 2018), while the shoreline normal fault (f2) of the island adds an extra 500–1000 (uncertain) m of normal displacement (Fig. 1c). Hence, altogether, the Alonnisos fault system has a normal displacement component in the order of 6–7 km.

It has been demonstrated, that precise datasets (e.g. elevation of dated marine terraces) and well-constrained fault properties allow for the application of sophisticated fault model setups (de Gelder et al., 2019). However, in our case, the datasets used for the model setup (estimated fault geometry) and validation (shortening and tilt angle estimations) are significantly less precise. For this reason, and based on the observations and considerations above, we designed an elastic half-space model with a single rectangular dislocation and assuming uniform slip, which allows to compare the first order characteristics of models and observations. The dislocation is 30 km long, has a dip angle varying between 55°, 60°, 65°, and 70°, and a vertical displacement component varying between 6 and 7 km. The dislocation extends from the surface to the depth of 10 km. We further adjusted the rake (slip vector direction) in 10° increments to achieve lateral footwall motion in the order of 1 km, corresponding to the observed shortening between Alonnisos and Skopelos (Figs. 2a, c). Following initial tests, we used a rake of −120° in the reference model (a rake of −90° or − 180° means pure normal or pure dextral displacement, respectively). Lateral footwall and hangingwall motion together were used to determine the overall dextral displacement (sum lateral motion) along the dislocation. Variation in model parameters was implemented in separate model runs. For the Poisson's ratio of the elastic half-space we chose the value of $\nu = 0.25$, which is an average crustal value for orogenic belts (Zandt and Ammon, 1995), but also ran models with a Poisson's ratio of 0.35 in order to test the influence of this parameter on the results.

4.4. Model results

To compare the predicted footwall tilt angles with the observed dip data of the Messinian rocks, we defined the tilt angle in the models as the average dip of the uplifted surface along a 5 km section (roughly equalling the width of Alonnisos) measured away from the fault (Fig. 4c). Results show that the tilt angle of the footwall is proportional with the dip angle of the fault and the amount of vertical slip on the fault (Fig. 4e). The observed post-Messinian tilting of around 13–14° on Alonnisos is closely approximated by models with a dip of 65° and 6–7 km of vertical displacement, or a dip of 60° or 70° and a vertical displacement of 7 or 6 km, respectively (Fig. 4a, e). A dip of 70° and a

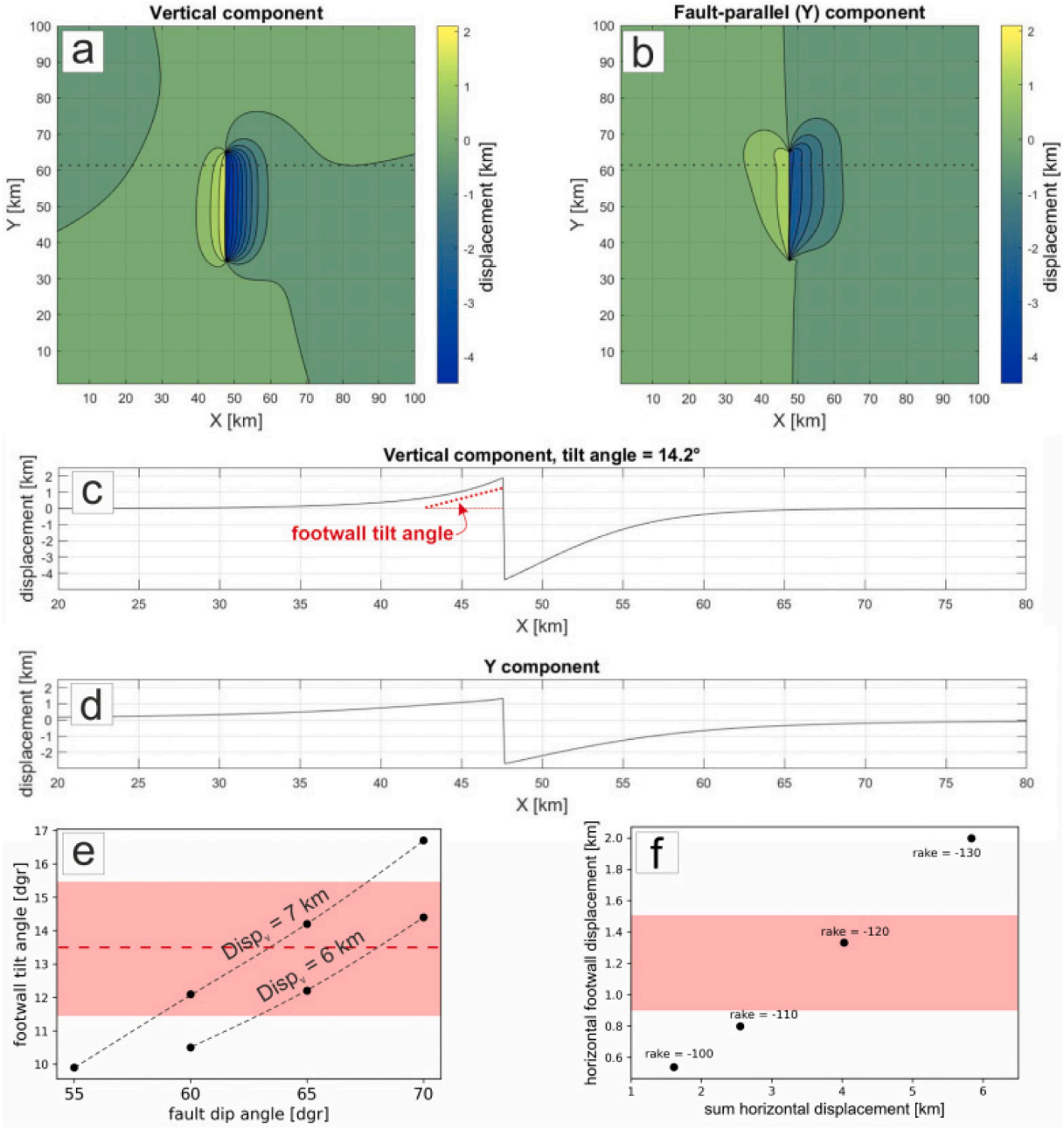

Fig. 4. Results of elastic half-space dislocation models (Okada, 1985; Nikkhoo et al., 2016). The reference model (plots a-d) has a fault dip angle of 65°, a vertical displacement component of 7 km, and a rake of −120° (where −90° is pure normal and − 180° is pure dextral displacement). **(a)** Map-view vertical displacement component of the reference model. Dashed line shows the trace of the cross-section plot on Fig. c. **(b)** Map-view fault-parallel (Y direction) displacement component of the reference model. Dashed line shows the trace of the cross-section plot on Fig. d. **(c)** Cross section (at Y = 62 km) plot of the vertical displacement component of the reference model. The footwall tilt angle (14.2°) is defined as the average dip of the first 5 km in the footwall measured from the dislocation. **(d)** Cross section (at Y = 62 km) plot of the fault-parallel (Y direction) displacement component of the reference model. **(e)** Footwall tilt angle as the function of the fault dip angle and the amount of vertical displacement ($Disp_v$) in various models. Connected dots are model results with the same amount of vertical displacement. Red dashed line represents the observed (average) tilt angle of the Messinian rocks (13.5°). Data points within the red area are model results that closely approximate the observed tilt angle (within 13.5 ± 2°). **(f)** Horizontal footwall displacement as a function of sum (footwall + hangingwall) horizontal displacement in models with various rake values. The horizontal displacement increases with decreasing rake (i.e. with increasing dextral slip component along the dislocation). The red area highlights the estimated 0.9–1.5 km, post-Messinian shortening at the termination zone of the Alonnisos fault. (For interpretation of the references to colour in this figure legend, the reader is referred to the web version of this article.)

vertical displacement of 7 km predicts an average tilt angle of almost 17°, which is significantly larger than the observations (Fig. 4e). Significantly smaller tilt angles are predicted by models with a dip of 55° or smaller and for models with a vertical displacement of <6 km.

Models show that a dextral displacement component (the sum of lateral footwall and hangingwall motion) of 3–4 km is required to achieve the inferred 900–1500 m fault-parallel motion in the footwall (Fig. 4f). This dextral displacement requires that the rake of the modelled dislocation is ca. -115° - -120° (Fig. 4f). The majority of the lateral slip component is accommodated in the hangingwall due to the dip of the fault (Fig. 4b, d, f). In the reference model, the footwall moves ~1.3 km in the positive Y direction (which could correspond to 1.3 km shortening at the fault termination zone in nature), while the hangingwall moves 2.7 km in the negative Y direction, resulting in a sum horizontal displacement of 4 km (Fig. 4b, d, f). Testing the Poisson's ratio ($\nu = 0.25$ in all of the models on Fig. 4e) showed a negligible influence on the results: using $\nu = 0.35$ instead of $\nu = 0.25$ resulted in a tilt angle increase of 0.2°, and increased the horizontal hangingwall displacement by 50 m.

In summary of the model results, the initial field-based conditions (a footwall tilt angle of 13–14° and a lateral footwall motion of 0.9–1.5 km) were predicted by models with a fault dip angle of 60–65°, a vertical displacement component of 6–7 km, and a dextral displacement component of 3–4 km.

5. Discussion

5.1. Normal faulting in the Sporades Basin

Model results show, that the 13–14° tilting of the Messinian strata can be explained by footwall uplift during normal slip on the Alonnisos fault system (f1 and f2 faults, Figs. 1b, c), i.e. during the deepening of the Sporades Basin. The required 6–7 km of vertical displacement on the Alonnisos fault system and the 60–65° fault dip angle are within uncertainties and consistent with observations and constraints from seismic data (Beniest et al., 2016; Sakellariou et al., 2016; Ferentinos et al., 2018). We note that fault segments with lower dip angles and listric geometry also exist along the Alonnisos fault (Ferentinos et al., 2018), which were not taken into account in our model setup. Nevertheless, the first-order agreement between observations and model predictions confirms that 1) the Neogene evolution of the Sporades Basin was dominated by extension, and 2) the Alonnisos fault is originally a major normal fault that controlled the subsidence of the Sporades Basin. These implications are in agreement with previous interpretations (Mascle and Martin, 1990; Beniest et al., 2016; Ferentinos et al., 2018). Our results furthermore highlight that the majority of extension and subsidence in the Sporades Basin has to be post-Messinian rather than early Miocene or Late Paleogene (while not excluding the possibility of minor pre-Messinian extension); this is the only way to achieve the 13–14° tilt angle in the Messinian rocks. This poses additional constraints to basin evolution models that are based on seismic datasets hindered by the lack of local borehole control and the strong Messinian salt reflection preventing the proper imaging of the underlying older sediments (Beniest et al., 2016; Sakellariou et al., 2016; Ferentinos et al., 2018). Dominantly Late Miocene and post-Miocene extension in the Sporades Basin as suggested by our results is consistent with the interpretation of Sakellariou et al. (2016) and Ferentinos et al. (2018). However, the new timing constraint is less consistent with the interpretation of up to 1 km thick Paleogene and Lower Miocene deposits extrapolated into the Sporades Basin by Beniest et al. (2016), or the interpretation of initial Paleogene basin development adjacent to the Northern Sporades by Porkoláb et al. (2019) and Porkoláb et al. (2020). While extension has probably been active on the Northern Sporades since late Paleogene times (Porkoláb et al., 2020), the deepening of the Sporades Basin appears to be a substantially younger, post-Messinian process.

5.2. Dextral faulting in the Sporades Basin

Field observations and structural analysis show that ~1 km shortening was accommodated by gentle folding at the termination zone of the Alonnisos fault. The NNW-SSE orientation of the gentle folds suggest ENE-WSW oriented shortening, which corresponds reasonably well with the E-W shortening and perpendicular extension directions derived from strain rate tensor calculations based on GNSS data (Hollenstein et al., 2008; Müller et al., 2013). Observations supported by model results furthermore imply that the ~1 km shortening is related to dextral slip on the Alonnisos fault system. Reflection seismic data and structural analysis up to now have not shown evidence for major dextral reactivations on the Alonnisos fault system (e.g. Ferentinos et al., 2018). In addition, focal mechanism solutions suggest that dextral slip events are currently distributed across the whole Sporades Basin (and NAT) rather than being focussed along the Alonnisos fault system (e.g. close to f3, Fig. 1b, Kapetanidis and Kassaras, 2019; Kassaras et al., 2020). Consequently, the identification and estimation of significant dextral slip on the Alonnisos fault system are critical new inferences for the tectonic evolution of the area. Model results imply that the required ~1 km of lateral footwall motion towards the SW (causing the shortening) could have been achieved by 3–4 km of dextral slip, with the majority of the lateral motion taking place in the hangingwall of the fault (Figs. 4 b, d, f). Our results hence suggest that the observed shortening on SW-Alonnisos and SE-Skopelos corresponds to a dextral displacement of 3–4 km along the Alonnisos fault system. Using the current rate of fault-parallel convergence between Alonnisos and Skopelos islands (~ 7 mm/yr, calculated from Hollenstein et al., 2008), the ~1 km shortening that we observed would take ~150 kyr to accumulate. This time frame would also be roughly consistent with the model results of Müller et al. (2013), which implies a current displacement rate of 5–15 mm/yr for the NAF in the Sporades Basin. This first order approximation shows that the propagation of the NAF into the Sporades Basin and especially the dextral slip on the Alonnisos fault system is likely very young. It has been proposed, that the propagation of the NAF into the NAT might be Early-Middle Pleistocene (Roussos and Lyssimachou, 1991; Beniest et al., 2016; Brun et al., 2016). Based on our estimations, the initiation of dextral movements in the Sporades Basin could be even younger, Late Pleistocene. Alternatively, an initially slow dextral slip could have been accelerating since the Early-Middle Pleistocene. In the former case, it is likely that "pure" normal faulting along the Alonnisos fault system was replaced by dominantly dextral slip during the Late Pleistocene, while the latter case would allow for initially slow, possibly oblique normal-dextral faulting from the Early-Middle Pleistocene, gradually evolving into a pure dextral system that is inferred presently by GNSS and seismological data (e.g. Hatzfeld et al., 1999; Kiratzi, 2002; Kiratzi and Louvari, 2003; Hollenstein et al., 2008; Kassaras et al., 2020).

5.3. Propagation of the NAF: regional implications

The NAF has a dextral displacement of ~85 km at the Sea of Marmara (Armijo et al., 1999), ~ 300 km away from the Sporades Basin, where the dextral displacement is around 3–4 km on the largest fault structure (Alonnisos fault system, Fig. 1). This eastward decrease in the displacement could largely be attributed to the decreasing displacement towards the tip of a propagating strike-slip fault. However, as the occurrence of strike-slip earthquake focal mechanism solutions (e.g. Kassaras et al., 2020) and the structural analysis of bathymetry and seismic data in the NAT (Sakellariou et al., 2016) show, there is also a significantly wider distribution of dextral slip in the NAT compared to the NAF in Anatolia. While the Anatolian segment and the eastern NAT are characterized by a narrow (~ 10 km) zone of strike-slip earthquake locations defining a localized zone of deformation, the western NAT is characterized by an order of magnitude wider (~ 100 km) strike-slip-dominated deformation zone ranging from the Northern Sporades to the Chalkidiki peninsula (Fig. 1b, Kassaras et al., 2020). Consequently,

the dextral slip is distributed over numerous fault segments in the NAT, such that the related rock deformation is not recorded on Alonnisos and Skopelos. Furthermore, the regional occurrence of dextral earthquake focal mechanisms suggests that dextral displacement is distributed over a much larger area than the NAT itself, also including the more southern areas between Skyros and the Cyclades (Taymaz et al., 1991; Kiratzi and Louvari, 2003; Kassaras et al., 2020). The prime example of this is the dextral Skyros-Edremit Fault (Fig. 1a), which has a similar strike to the NAF and accommodates significant dextral slip in the Central Aegean region (currently up to 10 mm/yr as derived from GNSS-based modelling, Müller et al., 2013). The tectonic model of Armijo et al. (1996) accounted for such distributed dextral deformation by interpreting a southern splay of the NAF in the Aegean that connects into the Skyros basin. In contrast, significant dextral deformation South of the NAT appears to be inconsistent with other studies where the southern boundary fault of the NAT (including the Alonnisos fault) defines the boundary between a northern microplate dominated by strike-slip deformation and a southern, SW moving microplate with less internal deformation (e.g. McClusky et al., 2000; Nyst and Thatcher, 2004). In the context of these microplate models, our results confirm that the Alonnisos fault is an important strike-slip deformation zone.

A second mechanism that could contribute to the decrease of displacement towards the western NAT is stress transfer through the lithosphere. Stresses arising from the extrusion of Anatolia could also be transferred towards the Gulf of Corinth and Evvoia where predominantly extensional deformation has been localized into rift structures during the past Myr (e.g. Armijo et al., 1996; Faucher et al., 2021), or towards the Kephalonia-Lefkada transform fault (e.g. Kiratzi and Louvari, 2003; Le Pichon et al., 2016). A few studies furthermore argue that the propagation of the NAF into the Aegean already lead to the formation of a regional Aegean-Anatolian plate boundary, with the NAF fully accommodating the previously more distributed deformation (Le Pichon et al., 2016; Faucher et al., 2021). While the idea of the fully localized Aegean-Anatolia plate boundary might fit with the observed stress field changes during the Pleistocene in the North Aegean and Central Greece (Lybéris, 1984; Lyberis and Sauvage, 1985; Faucher et al., 2021), it is not supported by the seismological and structural data (Taymaz et al., 1991; Kiratzi and Louvari, 2003; Sakellariou et al., 2016; Kassaras et al., 2020). In contrast, these data suggest that deformation is not yet fully localized on a single major structure, showing agreement with our estimates of a modest 3–4 km of dextral slip component along the Alonnisos fault system.

The timing and kinematic characteristics of the NAF propagation from the Sea of Marmara into the NAT and mainland Greece are further key problems. Le Pichon et al. (2016) have shown that deformation at the Sea of Marmara was largely extensional between 5 and 2.5 Ma, resulting in the formation of a major extensional basin resembling the presently active Corinth rift. Since then the Sea of Marmara became a fully localized strike-slip plate boundary zone, which accommodated ~85 km of dextral slip (Armijo et al., 1999; Le Pichon et al., 2016). In the light of our results, the Sporades basin (and more widely the NAT) appears to be undergoing a similar evolution. It originated as an extensional basin with the main phase of deepening occurring within the last 5 Myrs (as evidenced by the substantially tilted Messinian strata), and was reactivated in dextral sense during the Pleistocene (Lybéris, 1984; Lyberis and Sauvage, 1985; Roussos and Lyssimachou, 1991; Beniest et al., 2016), possibly as recent as 150 kyr in our estimation. The pre-dextral origin of the NAT is further supported by the geometry of the NAF: the latter changes its strike from ENE-WSW to NE-SW when entering the NAT (Fig. 1a) implying that the reactivation of pre-existing structures was favoured over the formation of new dextral fault segments when the propagating NAF reached the NAT (e.g. Roussos and Lyssimachou, 1991). Although the Sporades Basin accommodated significantly less dextral motion than the Sea of Marmara up to present, the process of dextral shear localization is proceeding (e.g. Kassaras et al., 2020) and may develop into a dextral plate boundary, similar to the Sea of Marmara. Following this line of thought, one could speculate that the Evvoia and Corinth rifts, where extensional deformation has accelerated in the last Myr (Armijo et al., 1996) could be the next extensional basins that undergo substantial dextral strain localization in the future. Another possible future scenario involves the continuation of stress transfer to the Kephalonia - Lefkada transform fault, where dextral slip is already localized (Kiratzi and Louvari, 2003; Le Pichon et al., 2016). This latter could result in the formation of transfer faults through Central Greece, connecting a more localized NAF in the North Aegean with the Kephalonia - Lefkada transform fault, eventually forming a continuous plate boundary (e.g. Kiratzi and Louvari, 2003; Le Pichon et al., 2016).

6. Conclusions

The presented structural field data and analytical modelling revealed and quantified normal and dextral faulting at the boundary fault system of the Sporades Basin. The results of this study allowed to draw the following main conclusions:

- The Messinian rocks of Alonnisos record significant (~ 13.5°) tilting and gentle folding close to the termination zone of the Alonnisos fault.
- The tilting of the Messinian rocks implies footwall uplift as a response to normal faulting in the order of 6–7 km (vertical displacement) along Alonnisos fault system. This constrains the substantial deepening of the Sporades Basin for the last 5 Myr.
- Gentle post-Messinian folding accommodated ~1 km shortening at the footwall termination zone of the main fault, which implies that dextral slip in the order of 3–4 km occurred along the Alonnisos fault system, possibly during the last 100–200 kyr.
- Propagation of the dextral North Anatolian Fault into the North Aegean Trough reactivated major pre-existing normal faults in the Sporades Basin and is currently expressed by distributed dextral deformation across the North Aegean region.

CRediT authorship contribution statement

Kristóf Porkoláb: Conceptualization, Methodology, Software, Validation, Investigation, Visualization, Writing - original draft. **Ernst Willingshofer:** Investigation, Supervision, Project administration, Writing - review & editing. **Dimitrios Sokoutis:** Investigation, Supervision, Project administration, Writing - review & editing. **Eszter Békési:** Methodology, Writing - review & editing. **Fred Beekman:** Project administration, Writing - review & editing.

Declaration of Competing Interest

The authors declare the following financial interests/personal relationships which may be considered as potential competing interests: Kristof Porkolab reports financial support was provided by Horizon 2020.

Data availability

Data will be made available on request.

Acknowledgements

The research leading to these results has received funding from the European Union's MSCA-ITN-ETN Project SUBITOP 674899. We are grateful to two anonymous reviewers for the insightful and constructive suggestions.

References

Armijo, R., Meyer, B., King, G.C.P., Rigo, A., Papanastassiou, D., 1996. Quaternary evolution of the Corinth Rift and its implications for the Late Cenozoic evolution of the Aegean. Geophys. J. Int. 126 (1), 11–53. https://doi.org/10.1111/j.1365-246X.1996.tb05264.x.

Armijo, R., Meyer, B., Hubert, A., Barka, A., 1999. Westward propagation of the North Anatolian fault into the northern Aegean: timing and kinematics. Geology 27 (3), 267–270. https://doi.org/10.1130/0091-7613(1999)027<0267:Wpotna>2.3.Co;2.

Barka, A., 1992. The North Anatolian Fault Zone, Paper Presented at Annales Tectonicae.

Beniest, A., Brun, J.P., Gorini, C., Crombez, V., Deschamps, R., Hamon, Y., Smit, J., 2016. Interaction between trench retreat and Anatolian escape as recorded by neogene basins in the northern Aegean Sea. Mar. Pet. Geol. 77, 30–42. https://doi.org/10.1016/j.marpetgeo.2016.05.011.

Brooks, M., Ferentinos, G., 1980. Structure and evolution of the Sporadhes basin of the North Aegean trough, northern Aegean Sea. Tectonophysics 68 (1–2), 15–30.

Brun, J.P., Sokoutis, D., 2007. Kinematics of the southern rhodope core complex (North Greece). Int. J. Earth Sci. 96 (6), 1079–1099. https://doi.org/10.1007/s00531-007-0174-2.

Brun, J.-P., Faccenna, C., Gueydan, F., Sokoutis, D., Philippon, M., Kydonakis, K., Gorini, C., 2016. The two-stage Aegean extension, from localized to distributed, a result of slab rollback acceleration 1. Can. J. Earth Sci. 53 (11), 1142–1157.

de Gelder, G., Fernandez-Blanco, D., Melnick, D., Duclaux, G., Bell, R.E., Jara-Munoz, J., Armijo, R., Lacassin, R., 2019. Lithospheric flexure and rheology determined by climate cycle markers in the Corinth Rift. Sci. Rep. 9 (1), 4260. https://doi.org/10.1038/s41598-018-36377-1.

Faucher, A., Gueydan, F., Jolivet, M., Alsaif, M., Celerier, B., 2021. Dextral strike-slip and normal faulting during middle Miocene Back-Arc extension and westward Anatolia extrusion in Central Greece. Tectonics 40 (6) e2020TC006615.

Ferentinos, G., Georgiou, N., Christodoulou, D., Geraga, M., Papatheodorou, G., 2018. Propagation and termination of a strike slip fault in an extensional domain: the westward growth of the North Anatolian Fault into the Aegean Sea. Tectonophysics 745, 183–195. https://doi.org/10.1016/j.tecto.2018.08.003.

Hatzfeld, D., Ziazia, M., Kementzetzidou, D., Hatzidimitriou, P., Panagiotopoulos, D., Makropoulos, K., Papadimitriou, P., Deschamps, A., 1999. Microseismicity and focal mechanisms at the western termination of the North Anatolian Fault and their implications for continental tectonics. Geophys. J. Int. 137 (3), 891–908. https://doi.org/10.1046/j.1365-246x.1999.00851.x.

Hollenstein, C., Muller, M.D., Geiger, A., Kahle, H.G., 2008. Crustal motion and deformation in Greece from a decade of GPS measurements, 1993-2003. Tectonophysics 449 (1–4), 17–40. https://doi.org/10.1016/j.tecto.2007.12.006.

Hubert-Ferrari, A., Armijo, R., King, G., Meyer, B., Barka, A., 2002. Morphology, displacement, and slip rates along the North Anatolian Fault, Turkey. J. Geophys. Res. Solid Earth 107 (B10). ETG 9-1-ETG 9-33.

Jacobshagen, V., Matarangas, D., 2004. Nappe structure of the North Sporades (Greece): on the geological evolution of Alonnisos Island. Δελτίον της Ελληνικής Γεωλογικής Εταιρίας 36 (4), 1636–1642.

Jacobshagen, V., Wallbrecher, E., 1984. Pre-Neogene nappe structure and metamorphism of the North Sporades and the southern Pelion peninsula. Geol. Soc. Lond., Spec. Publ. 17 (1), 591–602.

Jolivet, L., Brun, J.P., 2010. Cenozoic geodynamic evolution of the Aegean. Int. J. Earth Sci. 99 (1), 109–138. https://doi.org/10.1007/s00531-008-0366-4.

Jolivet, L., et al., 2013. Aegean tectonics: Strain localisation, slab tearing and trench retreat. Tectonophysics 597, 1–33. https://doi.org/10.1016/j.tecto.2012.06.011.

Kapetanidis, V., Kassaras, I., 2019. Contemporary crustal stress of the Greek region deduced from earthquake focal mechanisms. J. Geodyn. 123, 55–82. https://doi.org/10.1016/j.jog.2018.11.004.

Kassaras, I., Kapetanidis, V., Ganas, A., Tzanis, A., Kosma, C., Karakonstantis, A., Valkaniotis, S., Chailas, S., Kouskouna, V., Papadimitriou, P., 2020. The New Seismotectonic Atlas of Greece (v1.0) and its implementation. Geosciences 10 (11), 447. ARTN 447. https://doi.org/10.3390/geosciences10110447.

Kelepertsis, A., 1974. Geological structure of Alonnisos and Peristera islands (Aegaean Sea, Greece). Z. Dtsch. Geol. Ges. 225–236.

Kiratzi, A.A., 2002. Stress tensor inversions along the westernmost North Anatolian Fault Zone and its continuation into the North Aegean Sea. Geophys. J. Int. 151 (2), 360–376. https://doi.org/10.1046/j.1365-246X.2002.01753.x.

Kiratzi, A., Louvari, E., 2003. Focal mechanisms of shallow earthquakes in the Aegean Sea and the surrounding lands determined by waveform modelling: a new database. J. Geodyn. 36 (1–2), 251–274. https://doi.org/10.1016/S0264-3707(03)00050-4.

Le Pichon, X., Angelier, J., Osmaston, M., Stegena, L., 1981. The Aegean Sea [and Discussion]. Philos. Trans. Royal Soc. London A Math. Phys. Eng. Sci. 300 (1454), 357–372.

Le Pichon, X., Şengör, A.C., Kende, J., İmren, C., Henry, P., Grall, C., Karabulut, H., 2016. Propagation of a strike-slip plate boundary within an extensional environment: the westward propagation of the North Anatolian Fault. Can. J. Earth Sci. 53 (11), 1416–1439.

Lybéris, N., 1984. Tectonic evolution of the North Aegean trough. Geol. Soc. Lond., Spec. Publ. 17 (1), 709–725.

Lyberis, N., Sauvage, J., 1985. Evolution tectonique de la région nord égéenne (Grece) du Pliocene au Pleistocene. Bull. Soc. Géol. France 1 (4), 581–595.

Mascle, J., Martin, L., 1990. Shallow structure and recent evolution of the Aegean Sea - a synthesis based on continuous reflection profiles. Mar. Geol. 94 (4), 271–299. https://doi.org/10.1016/0025-3227(90)90060-W.

Matarangas, D., 1992. Geological Investigation of Skopelos Island. North Sporades, Greece, Forschungszentrum Jülich, Zentralbibliothek.

McClusky, S., et al., 2000. Global Positioning System constraints on plate kinematics and dynamics in the eastern Mediterranean and Caucasus. J. Geophys. Res. Solid Earth 105 (B3), 5695–5719. https://doi.org/10.1029/1996jb900351.

McKenzie, D., 1972. Active tectonics of the Mediterranean region. Geophys. J. Int. 30 (2), 109–185.

McNeill, L.C., Mille, A., Minshull, T.A., Bull, J.M., Kenyon, N.H., Ivanov, M., 2004. Extension of the North Anatolian Fault into the North Aegean Trough: evidence for transtension, strain partitioning, and analogues for Sea of Marmara basin models. Tectonics 23 (2). https://doi.org/10.1029/2002tc001490. Artn Tc2016.

Müller, M., Geiger, A., Kahle, H.-G., Veis, G., Billiris, H., Paradissis, D., Felekis, S., 2013. Velocity and deformation fields in the North Aegean domain, Greece, and implications for fault kinematics, derived from GPS data 1993–2009. Tectonophysics 597, 34–49.

Nikkhoo, M., Walter, T.R., Lundgren, P.R., Prats-Iraola, P., 2016. Compound dislocation models (CDMs) for volcano deformation analyses. Geophys. J. Int. 208 (2), 877–894. https://doi.org/10.1093/gji/ggw427.

Nyst, M., Thatcher, W., 2004. New constraints on the active tectonic deformation of the Aegean. J. Geophys. Res. Solid Earth 109 (B11). https://doi.org/10.1029/2003jb002830. Artn B11406.

Okada, Y., 1985. Surface deformation due to shear and tensile faults in a half-space. Bull. Seismol. Soc. Am. 75 (4), 1135–1154. ://WOS:A1985ANX6800014.

Philippon, M., Brun, J.P., Gueydan, F., Sokoutis, D., 2014. The interaction between Aegean back-arc extension and Anatolia escape since Middle Miocene. Tectonophysics 631, 176–188. https://doi.org/10.1016/j.tecto.2014.04.039.

Porkoláb, K., Willingshofer, E., Sokoutis, D., Creton, I., Kostopoulos, D., Wijbrans, J., 2019. Cretaceous-Paleogene Tectonics of the Pelagonian zone: inferences from Skopelos Island (Greece). Tectonics 38 (6), 1946–1973. https://doi.org/10.1029/2018tc005331.

Porkoláb, K., Willingshofer, E., Sokoutis, D., Wijbrans, J., 2020. Strain localization during burial and exhumation of the continental upper crust: a case study from the Northern Sporades (Pelagonian thrust sheet, Greece). Glob. Planet. Chang. 194, 103292.

Poulimenos, G., Karkanas, P., 1998. Messinian carbonate and alluvial fan sedimentation in Alonnisos Island, Greece: sedimentary response to basement controls, inversion tectonics and climatic fluctuations. Geol. J. 33 (3), 159–175. ://WOS:000078131500003.

Roussos, N., Lyssimachou, T., 1991. Structure of the Central North Aegean Trough: an active strike-slip deformation zone. Basin Res. 3 (1), 37–46.

Sakellariou, D., Rousakis, G., Vougioukalakis, G., Ioakim, C., Panagiotopoulos, I., Morfis, I., Zimianitis, E., Athanasoulis, K., Tsampouraki-Kraounaki, K., Mpardis, D., 2016. Deformation pattern in the western North Aegean trough: preliminary results. Bull. Geol. Soc. Greece 50 (1), 124–133.

Şengör, A., Tüysüz, O., Imren, C., Sakınç, M., Eyidoğan, H., Görür, N., Le Pichon, X., Rangin, C., 2005. The North Anatolian fault: a new look. Annu. Rev. Earth Planet. Sci. 33, 37–112.

Taymaz, T., Jackson, J., Mckenzie, D., 1991. Active Tectonics of the North and Central Aegean Sea. Geophys. J. Int. 106 (2), 433–490. https://doi.org/10.1111/j.1365-246X.1991.tb03906.x.

Varesis, A., Anastasakis, G., 2021. Cenozoic marine basin evolution in the Western North Aegean trough margin: seismic stratigraphic evidence. Water 13 (16), 2267. ARTN 2267. https://doi.org/10.3390/w13162267.

Weissel, J.K., Karner, G.D., 1989. Flexural uplift of rift flanks due to mechanical unloading of the lithosphere during extension. J. Geophys. Res. Solid Earth Planets 94 (B10), 13919–13950. https://doi.org/10.1029/JB094iB10p13919.

Zandt, G., Ammon, C.J., 1995. Continental crust composition constrained by measurements of crustal Poisson's ratio. Nature 374 (6518), 152–154.